TECHNICAL ARTICLE

Multi-stage Single-Point Incremental Forming: An Experimental Investigation of Surface Roughness and Forming Time

Nikhil Bari and Shailendra Kumar

This paper describes an experimental investigation of surface roughness and forming time of parts formed by multi-stage single-point incremental forming (MSPIF). Process parameters, namely tool size, feed rate, step depth, sheet thickness, and spindle speed, are considered in the present study. Experiments are designed using the central composite design (CCD) method. Analysis of variance (ANOVA) is used to identify significance of process parameters for surface roughness and forming time. It is found that tool size is the most significant process parameter followed by step depth, spindle speed and sheet thickness for influencing surface roughness. Surface roughness initially decreases and then increases with increase in tool size. It decreases with decrease in step depth, spindle speed and sheet thickness. For forming time, step depth and feed rate are found significant. Forming time decreases with increase in step depth and feed rate. Regression models of surface roughness and forming time are also developed. Further, process parameters are optimized to minimize surface roughness and forming time of parts.

1. Introduction

Incremental sheet forming (ISF) is mainly used for small batch production of customized sheet metal parts. This technique is also known as die-less forming as it does not require die and punch setup to form a part. Higher formability is achieved in ISF than conventional sheet forming due to localized deformation (Ref 1, 2). Based on the number of contact point, ISF process is classified as single-point incremental forming (SPIF) and two-point incremental forming (TPIF). It is performed either in single stage or multi-stages. In multi-stage single-point incremental forming (MSPIF), part is formed using a single-point tool in more than one stage. Using this process, even the parts having high wall angle can be formed easily since the deformation zone is extended over a larger region of the part (Ref 3). As depicted in Fig. 1, final wall angle (θ_f) is formed with intermediate stages of wall angles θ_1 and θ_2. In MSPIF process, uniform thickness distribution is obtained in the formed part. Strength and formability of sheet metal part increase with increase in number of stages (Ref 4, 5). This process is used in forming of parts for various industrial and medical applications such as automobile headlight reflector (Ref 6), titanium skull implant (Ref 3), ankle support (Ref 7), fender car body (Ref 8), hole flanging (Ref 9,

10) and car tail light bracket (Ref 11). But poor geometrical accuracy, high surface roughness and forming time are major challenges in this process (Ref 12).

Some researchers have investigated formability, thickness distribution and geometrical accuracy of parts formed by MSPIF process. For example, Kim and Yang (Ref 3) studied the formability of conical cups using two-stage forming. Vertbert et al. (Ref 13) investigated thickness distribution of parts and concluded that this process gives a uniform thickness distribution. Malhotra et al. (Ref 14) and Manco et al. (Ref 15) examined the effect of tool path trajectory on formability of MSPIF. Li et al. (Ref 16) developed a mathematical expression to determine principle strains in formed parts. Liu et al. (Ref 17) reported the effect of multi-stage forming on thinning band and found that the thinning band in SPIF can be delayed in MSPIF process. Some researchers (Ref 18, 19) compared the forming limit curve (FLC) of SPIF with MSPIF and reported that the FLC of MSPIF is more uniform. Li et al. (Ref 19) analyzed the effect of stepping rate on geometrical accuracy and concluded that the geometrical accuracy increases with increase in stepping rate. Nirala et al. (Ref 20 and 21) have made efforts to increase the geometrical accuracy of parts by formed by MSPIF process using bottom forming toolpath strategy. Shamsari et al. (Ref 22) examined the formability of a two-stage SPIF for maximum forming depth. It is observed that two-stage forming enhances forming depth up to 26% as compared to SPIF. Dai et al. (Ref 23) studied the effect of feed rate, spindle speed and step depth on geometric accuracy of parts formed by MSPIF and concluded that step depth is the most influencing process parameter. Ndip et al. (Ref 24) formed a 75^0 wall angle in seven stages with the combination of outside-in (OI) and inside-out (IO) tool path.

Very limited study (Ref 25, 26) has been reported on the surface roughness of parts formed by MSPIF process. Skjoedt et al. (Ref 25) concluded that surface roughness increases with

Nikhil Bari and **Shailendra Kumar**, Departmant of Mechanical Engineering, Sardar Vallabhbhai National Institute of Technology, Surat, India. Contact e-mail: skbudhwar@med.svnit.ac.in.
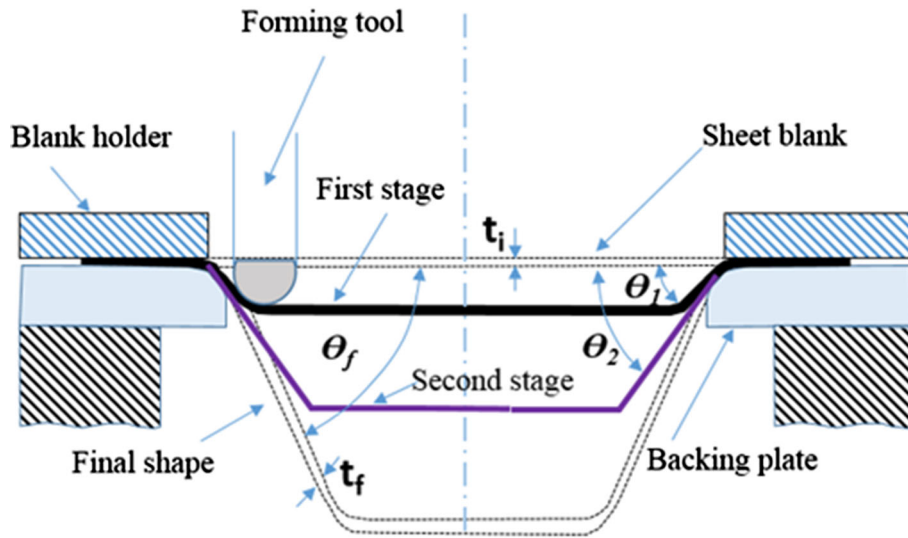
Fig. 1 Schematic of MSPIF

increase in number of stages. Gajjar et al. (Ref 26) studied the influence of feed rate, step depth and number of stages on surface roughness and concluded that the number of stages and step depth have considerable influence.

From the literature review, it is found that there is a stern need to investigate surface roughness and forming time of parts formed by MSPIF process (Ref 27). The present work is an effort to fulfill the above research gap. The subsequent section describes experimental plan of the present work.

2. Experimental Plan

Experiments are performed on a 3-axis CNC vertical milling machine (Make: Batliboi Ltd., India). To hold the blank on machine bed during MSPIF process, a fixture is designed and fabricated. This fixture consists of four hollow bars which serve as vertical columns. Sheet blank is clamped using two plates, i.e., top plate and bottom plate, as depicted in Fig. 2. For the present study, three hemispherical tools of diameter 8, 10 and 12 mm are designed and fabricated. The tool material is M2-grade high-speed high-chromium steel as it offers good wear resistance due to high chromium content. Sheet material is aluminum 1050 alloy. Initial surface roughness of blank and tool as measured with surface roughness tester (make: Mitu-toyo, Japan) is found as 0.278 and 0.133 μm, respectively. To reduce friction, hydraulic EP-90 oil is used as a lubricant during process.

In the present work, a conical frustum of 100 mm top diameter and 40 mm depth is fabricated as shown in Fig. 3(a). The final wall angle of 60^0 is obtained using a four-stage MSPIF process. The initial wall angle is 45^0, and at each stage it is increased by 5^0 (Ref 21, 28). For forming in each stage, the spiral toolpath strategy is used since it results in good surface finish (Ref 29, 30). Simulation of tool path is shown in Fig. 3(b). Methodology adopted for toolpath generation is depicted in Fig. 4. First of all, CAD models of conical frustum for each wall angle (45^0, 50^0, 55^0 and 60^0) are prepared. Then using digitized shape editor toolbox of CATIA (version: V5R21), slicing of each '.STL' file is performed and point
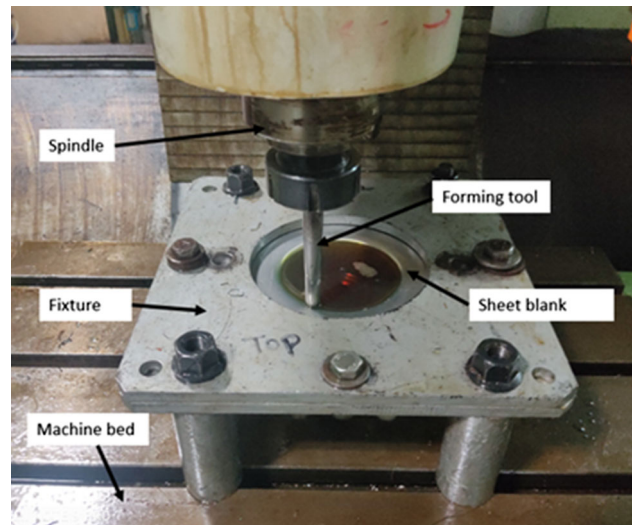

Fig. 2 Experimental setup

cloud data for each wall angle is extracted. Next, merging of all point cloud data is done in such a way that at the first stage cone with wall angle of 45^0 is formed, and then in subsequent stages wall angle is increased by 5^0. The merging of point cloud data and toolpath generation is done using MATLAB (version: 2020a). The generated toolpath is fed to controller of CNC milling machine for forming of parts.

Levels of process parameters (Table 1) for the present experimental study are selected on the basis of literature review (Ref 31, 32), trial experiments and available experimental setup. Experiments are designed as per face-centered composite design (CCD) of response surface methodology (RSM). The CCD method has high reliability for optimization and regression models (Ref 33). A three-level 5-factor quadratic model is chosen for the study. Design-expert 11 (Stat-Ease Inc.) software is used to design the experiments. Total 48 experiments including six experiments with center points, thirty six experiments at the factorial points and six experiments at the axial points are performed as given in Table 2.
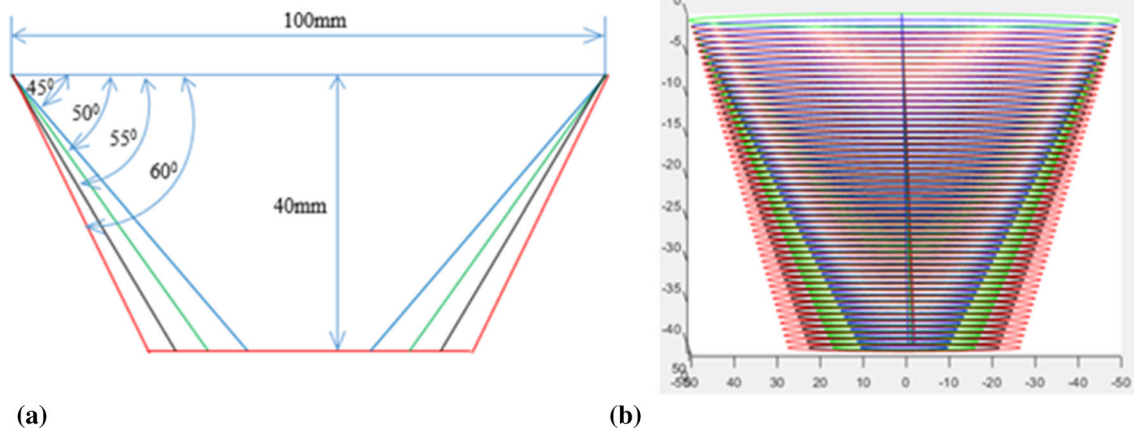
(a)

(b)

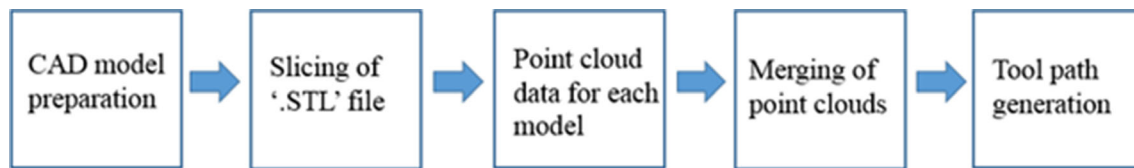**Fig. 3** (a) Part geometry; and (b) tool path for part geometry

Fig. 4 Procedure of toolpath generation for MSPIF process

Table 1 Process parameters with levels

Parameters	Levels		
	−1	0	1
Tool size (mm)	8	10	12
Feed rate (mm/min)	1000	1500	2000
Step depth (mm)	0.25	0.5	0.75
Sheet thickness (mm)	0.7	0.95	1.2
Spindle speed (RPM)	0	500	1000

After forming the parts, surface roughness of each part is measured using surface roughness tester (make: Mitutoyo, Japan). To increase accuracy of measurement, surface roughness is measured at eight distinct locations as depicted in Fig. 5, and average value of readings is taken. Forming time is noted from the display screen of CNC milling machine (Ref 30).

3. Results and Discussion

Measured values of surface roughness and forming time are given in Table 3. ANOVA is used to identify significance of process parameters and also to generate regression models. It gives statistical relationship between response and process parameters (Ref34).

3.1 Surface Roughness

ANOVA for surface roughness is given in Table 4. The R^2 analysis is used to determine robustness of ANOVA model. The value of R^2, R^2 (adj.) and R^2 (pred.) is 0.9683, 0.9449 and 0.8942, respectively, which are closed to 1. It indicates that the ANOVA model is mathematically valid. Confidence interval for the model is 95%, and hence terms having P value < 0.05 are significant terms. The SN (signal to noise) ratio is 21.85, which is greater than 4. It indicates adequate signal in the ANOVA model.

From ANOVA, it is found that tool size, step depth, spindle speed and sheet thickness are significant process parameters for influencing surface roughness.

3.1.1 Main Effect Plot for Surface Roughness. Main effect of the process parameters on the surface roughness (R_a) are plotted at the middle level (i.e., 0 level) in the design space as shown in Fig. 6. It is observed that the surface roughness initially decreases and then increases with increase in tool size (Fig. 6a). This is because with increase in tool size, overlapping impressions of tool in consecutive layers occur which results in reduced waviness and thus decrease in surface roughness. But with further increase in tool size, contact area of tool tip and blank increases which results in increased friction and wear and thus increase in surface roughness. Similar results were observed by Mulay et al. (Ref 31) and Dodiya et al. (Ref 32). It is also found that surface roughness increases with increase in step depth as shown in Fig. 6(c). With increase in step depth, scallop height is increased, which results in increased surface roughness. Also, at high step depth, chips stick to tool tip due to high friction, which results in increased surface roughness (Ref 31, 32, 34, 35, 36). Sheet thickness has very less effect on surface roughness (Ref 32, 37). Surface roughness increases slightly with increase in sheet thickness (Fig. 6d). It is also observed that spindle speed has very less effect on surface roughness. As shown in Fig. 6(e), surface roughness slightly increases with increase in spindle speed. This is because friction between tool and blank sheet surface increases with increase in spindle speed (Ref 38).

Table 2 Design of experiments

Test run	Tool size, mm	Feed rate, mm/min	Step depth, mm	Sheet thickness, mm	Spindle speed, RPM
1	12	2000	0.25	1.2	1000
2	8	1000	0.75	1.2	0
3	10	1500	0.75	0.95	500
4	8	1000	0.75	1.2	1000
5	12	1000	0.75	1.2	1000
6	8	2000	0.75	1.2	0
7	10	1500	0.5	0.95	500
8	12	2000	0.75	1.2	1000
9	10	2000	0.5	0.95	500
10	12	1000	0.75	0.7	1000
11	8	1000	0.25	1.2	1000
12	10	1500	0.25	0.95	500
13	12	1000	0.25	1.2	1000
14	12	1000	0.25	1.2	0
15	10	1500	0.5	1.2	500
16	8	2000	0.25	1.2	1000
17	8	2000	0.75	0.7	1000
18	8	2000	0.75	0.7	0
19	12	1500	0.5	0.95	500
20	10	1500	0.5	0.95	500
21	10	1500	0.5	0.95	1000
22	8	2000	0.25	1.2	0
23	8	1500	0.5	0.95	500
24	12	2000	0.75	0.7	0
25	10	1000	0.5	0.95	500
26	8	1000	0.75	0.7	0
27	10	1500	0.5	0.95	500
28	10	1500	0.5	0.95	500
29	12	2000	0.25	0.7	0
30	8	2000	0.25	0.7	0
31	10	1500	0.5	0.95	500
32	10	1500	0.5	0.95	500
33	12	1000	0.25	0.7	0
34	12	2000	0.75	1.2	0
35	12	1000	0.75	0.7	0
36	8	1000	0.25	1.2	0
37	8	1000	0.25	0.7	0
38	10	1500	0.5	0.95	0
39	8	2000	0.75	1.2	1000
40	8	2000	0.25	0.7	1000
41	8	1000	0.75	0.7	1000
42	8	1000	0.25	0.7	1000
43	12	1000	0.75	1.2	0
44	12	2000	0.25	0.7	1000
45	12	2000	0.75	0.7	1000
46	12	2000	0.25	1.2	0
47	12	1000	0.25	0.7	1000
48	10	1500	0.5	0.7	500

3.1.2 Response Surface Graphs of Interactions for Surface Roughness. It is observed from ANOVA (Table 4) that there are three interactions which influence surface roughness. The simultaneous interactive effect of two process parameters is analyzed through 3-D response surface graph by keeping rest of process parameters at middle levels. Interactions of process parameters are shown in Fig. 7. The response surface graph for interaction effect of tool size and step depth is shown in Fig. 7(a) and (b). It is observed that surface roughness decreases with simultaneous increase in tool size and step depth. Once the value of tool size crosses 10 mm, the surface

roughness becomes constant. The minimum value of surface roughness is observed at step depth of 0.25 mm and tool size of 11 mm. The maximum value of surface roughness is obtained at step depth of 0.75 mm and tool size of 8 mm. Tool size has more effect on surface roughness than step depth. It is found that large tool size with low step depth is required to reduce surface roughness.

The response surface plot of interaction for tool size and sheet thickness is depicted in Fig. 7(c) and (d). It is observed that the contour lines are nearly parallel along vertical direction indicating less effect of sheet thickness on surface roughness. Moreover, surface roughness continuously decreases with
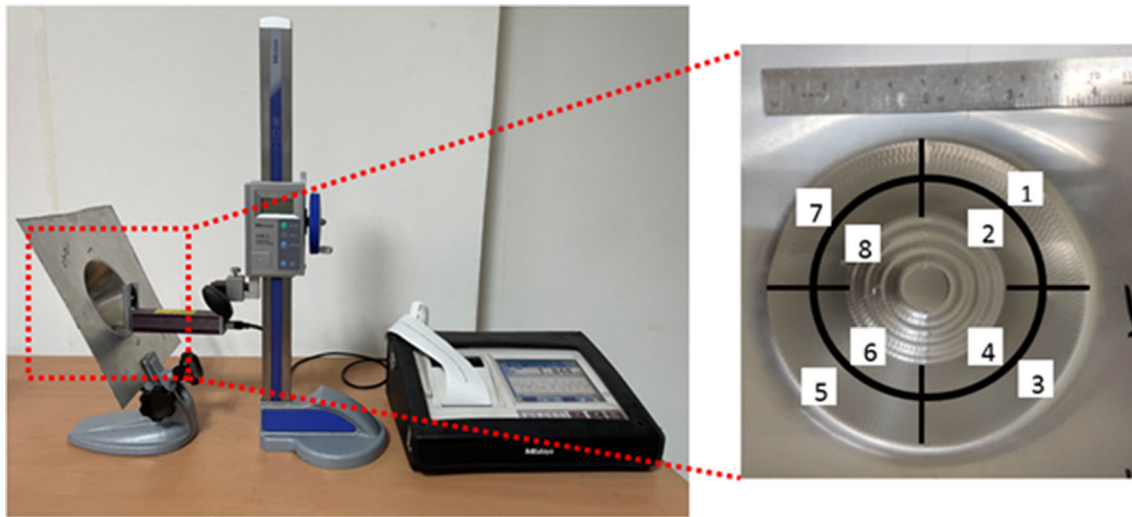
Fig. 5 Surface roughness measurement

Table 3 Measured values of responses

Test run	Surface roughness, R_a μm	Forming time, minute	Test run	Surface roughness, R_a μm	Forming time, minute
1	1.029	70.00	25	0.772	70.80
2	2.726	47.55	26	3.468	47.55
3	0.938	31.70	27	1.037	47.20
4	3.559	47.55	28	0.953	47.20
5	1.248	47.55	29	0.468	70.00
6	2.802	23.80	30	1.102	70.00
7	0.799	47.20	31	0.472	47.20
8	1.574	23.80	32	0.494	47.20
9	0.871	35.40	33	0.404	140.00
10	0.697	47.55	34	0.985	23.80
11	1.945	140.00	35	0.784	47.55
12	0.62	93.30	36	1.314	140.00
13	0.718	140.00	37	1.496	140.00
14	0.847	140.00	38	0.45	47.20
15	1.542	47.20	39	3.763	23.80
16	1.936	70.00	40	2.405	70.00
17	3.828	23.80	41	3.929	47.55
18	2.893	23.80	42	1.754	140.00
19	0.911	47.20	43	1.025	47.55
20	0.771	47.20	44	0.538	70.00
21	0.661	47.20	45	0.784	23.80
22	1.708	70.00	46	0.685	70.00
23	2.694	47.20	47	0.475	140.00
24	0.48	23.80	48	0.445	47.20

increase in tool size and sheet thickness simultaneously. The minimum value of surface roughness for interaction is 0.57 μm and observed at 10 mm tool size with 0.95 mm sheet thickness. However, maximum value of R_a is observed at 0.7 and 1.2 mm sheet thickness for 8 mm tool size. Hence it is inferred that large tool size combined with middle level of sheet thickness results in improved surface finish.

The combined effect of tool size and spindle speed is shown in Fig. 7(e) and (f). It is noted that contour lines are diverged at the upper right corner. Surface roughness decreases by increase in tool size and spindle speed simultaneously. For low value of spindle speed, surface roughness is reduced with increase in

tool size. The minimum value of R_a is found at zero RPM and 11 mm tool size. However, there is less effect of spindle speed at large tool size. Hence, large tool size with low spindle speed is required to reduce surface roughness.

3.2 Forming Time

The ANOVA for forming time is given in Table 5. The value of R^2, R^2 (adj.) and R^2 (pred.) is 0.9988, 0.9980 and 0.9957, respectively. Lack of fit is insignificant which implies that the model can be used to analyze the effect of process parameters on forming time. The SN (signal to noise) ratio is 94.883, which is greater than 4, indicating adequate signal in ANOVA

Table 4 ANOVA table for surface roughness

| Source	Sum of squares	Degrees of freedom	Mean squares	F-value	P-value	Remark
Model	48.98	20	2.45	41.28	<0.0001	Significant
A-Tool size	25.89	1	25.89	436.41	<0.0001	Significant
B-Feed rate	0.01	1	0.0140	0.2360	0.6310	Not significant
C-Step depth	7.57	1	7.57	127.53	<0.0001	Significant
D-Sheet thickness	0.35	1	0.3513	5.92	0.0219	Significant
E-Spindle speed	1.53	1	1.53	25.74	<0.0001	Significant
AB	0.0003	1	0.0003	0.0052	0.9433	Not significant
AC	3.71	1	3.71	62.52	<0.0001	Significant
AD	0.66	1	0.6621	11.16	0.0025	Significant
AE	0.55	1	0.5578	9.40	0.0049	Significant
BC	0.04	1	0.0484	0.8164	0.3742	Not significant
BD	0.08	1	0.0809	1.36	0.2531	Not significant
BE	0.19	1	0.1911	3.22	0.0839	Not significant
CD	0.01	1	0.0162	0.2738	0.6051	Not significant
CE	0.06	1	0.0651	1.10	0.3043	Not significant
DE	0.004	1	0.0042	0.0702	0.7931	Not significant
A^2	2.41	1	2.41	40.67	< 0.0001	Significant
B^2	0.0001	1	0.0001	0.0022	0.9630	Not significant
C^2	0.0031	1	0.0031	0.0517	0.8219	Not significant
D^2	0.08	1	0.0794	1.34	0.2575	Not significant
E^2	0.16	1	0.1654	2.79	0.1066	Not significant
Residual	1.60	27	0.0593			Not significant
Lack of Fit	1.33	22	0.0606	1.13	0.4945	Not significant
Pure Error	0.2691	5	0.0538			
Total	50.58	47				
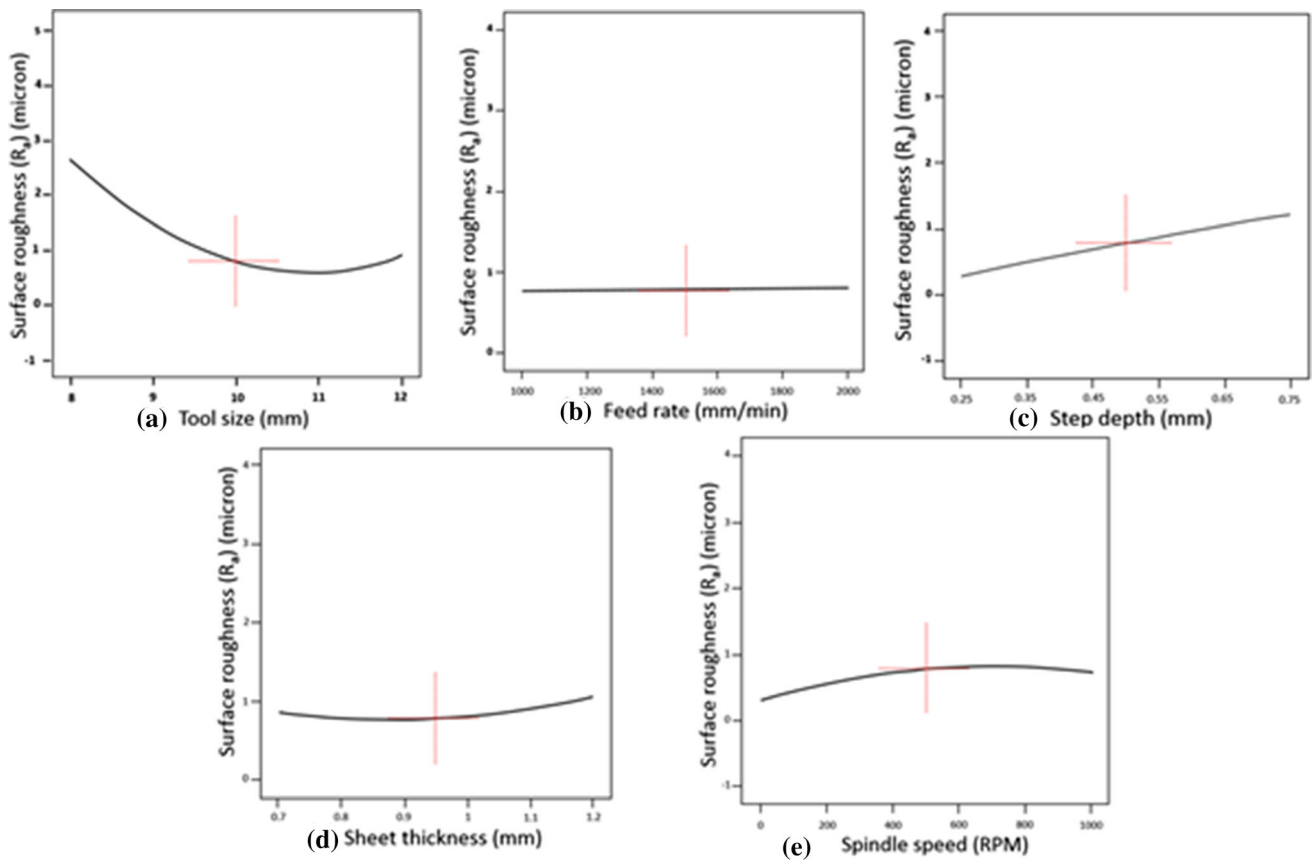
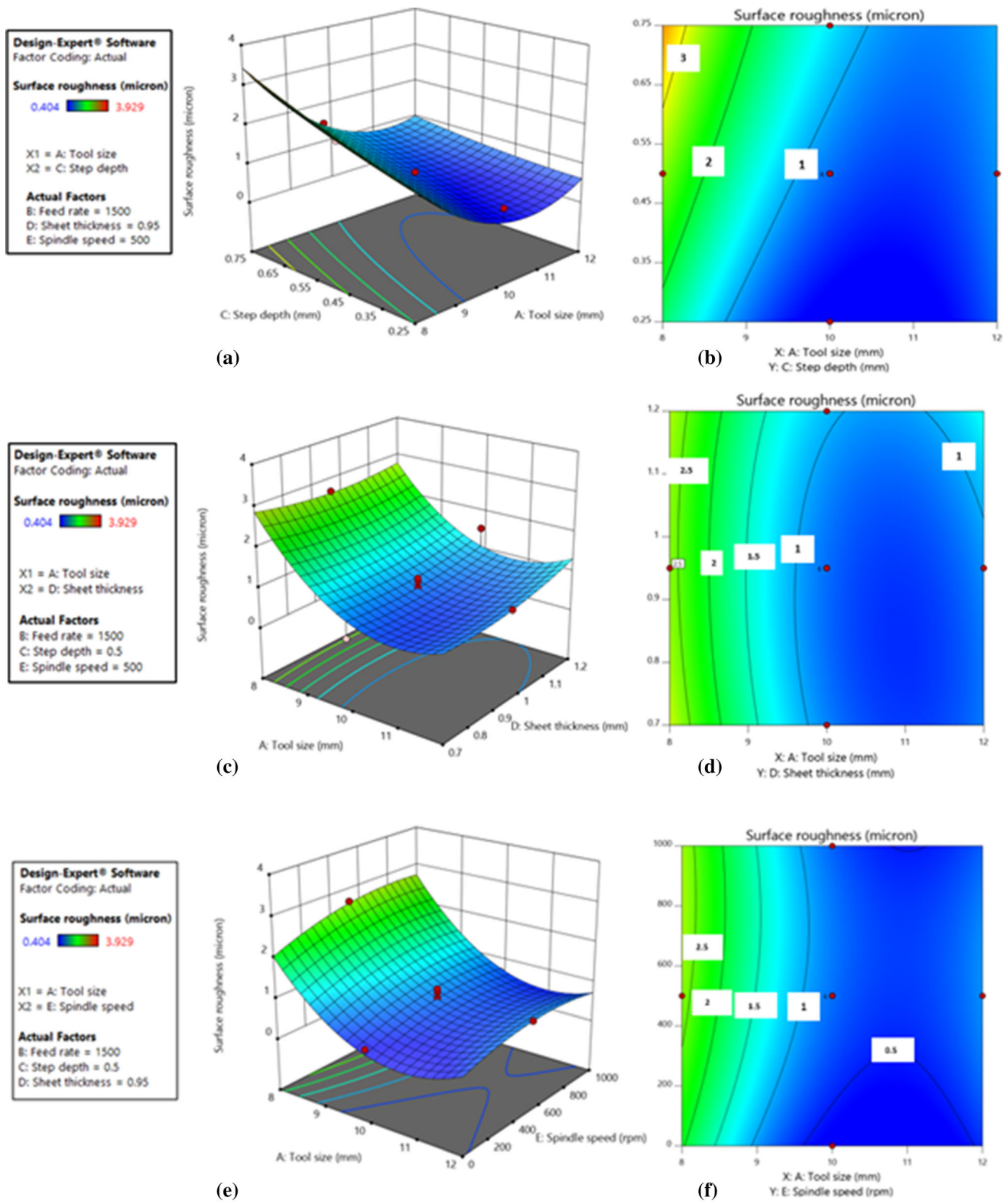Fig. 6 Main effect plot for surface roughness

Fig. 7 Response surface graph of interactions for surface roughness

model. Hence, this model can be used to navigate the design space.

From ANOVA, P value of step depth and feed rate is less than 0.05; therefore, both parameters are significant for forming time of MSPIF parts.

3.2.1 Main Effect Plot for Forming Time. Main effect of process parameters on the forming time is plotted at the middle level (i.e., 0 level) in the design space as depicted in Fig. 8. It is observed that forming time decreases with increase

Table 5 ANOVA table of forming time

| Source	Sum of squares	Degrees of freedom	Mean squares	F-value	P-value	Remarks
Model	67643.43	20	3382.17	1007.79	<0.0001	Significant
A-Tool size	0	1	0	0	1	Not significant
B-Feed rate	18154.37	1	18154.37	5409.50	<0.0001	Significant
C-Step depth	40323.32	1	40323.32	12015.23	<0.0001	Significant
D-Sheet thickness	0	1	0	0	1	Not significant
E-Spindle speed	0	1	0	0	1	Not significant
AB	0	1	0	0	1	Not significant
AC	0	1	0	0	1	Not significant
AD	0	1	0	0	1	Not significant
AE	0	1	0	0	1	Not significant
BC	4272.49	1	4272.49	1273.08	<0.0001	Significant
BD	0	1	0	0	1	Not significant
BE	0	1	0	0	1	Not significant
CD	0	1	0	0	1	Not significant
CE	0	1	0	0	1	Not significant
DE	0	1	0	0	1	Not significant
A^2	0.45	1	0.45	0.13	0.71	Not significant
B^2	99.02	1	99.02	29.50	<0.0001	Significant
C^2	611.41	1	611.41	182.18	<0.0001	Significant
D^2	0.45	1	0.45	0.13	0.71	Not significant
E^2	0.45	1	0.45	0.13	0.71	Not significant
Residual	90.61	27	3.35			Not significant
Lack of Fit	90.61	22	4.11			Not significant
Pure Error	0	5	0			
Total	67734.05	47				
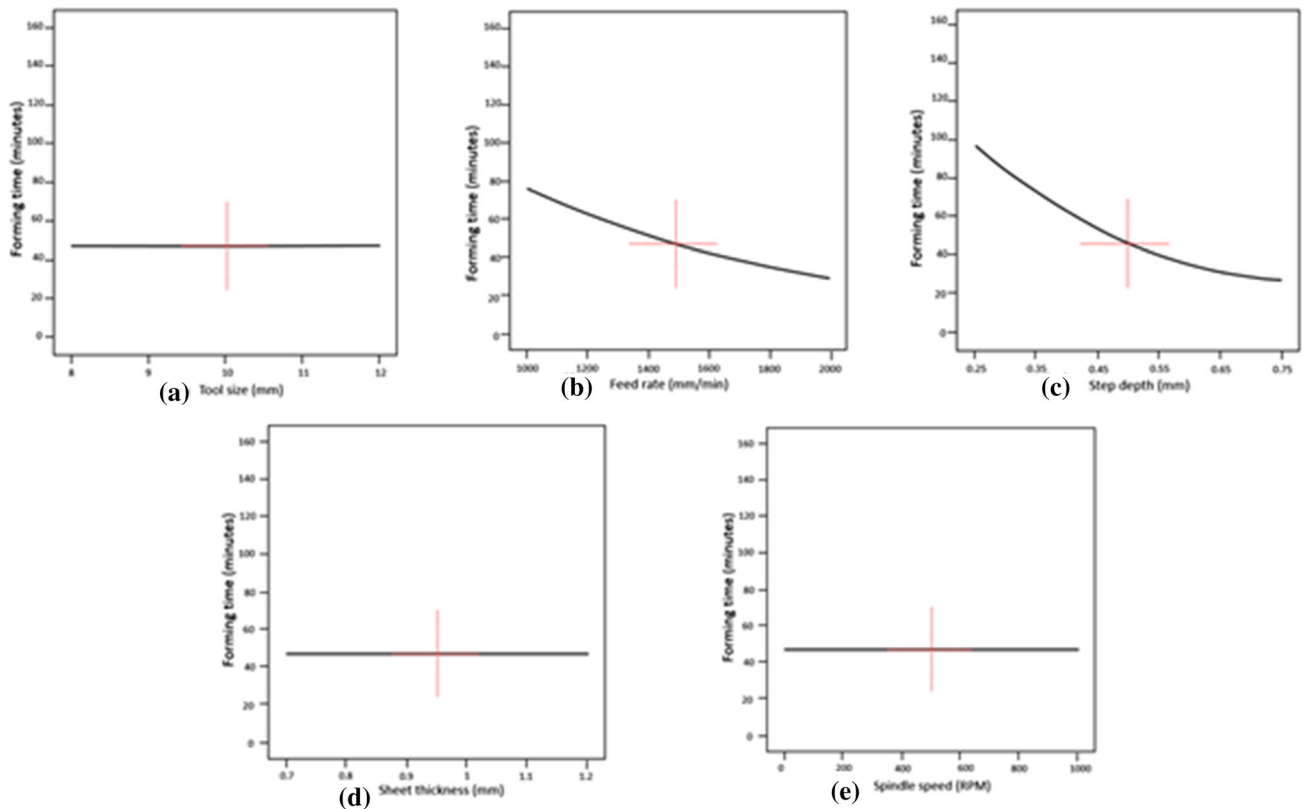
Fig. 8 Main effect plot for forming time

in feed rate. This is because as feed rate increases, tool moves with high velocity which results in decreased forming time. It is also found that forming time decreases with increase in step depth. This is because less number of horizontal contours are required to form parts.

3.2.2 Response Surface Graph of Interaction for Forming Time. From ANOVA (Table 5), it is observed that there is only one interaction which has significant effect on forming time of MSPIF parts. The simultaneous interactive effect of feed rate and step depth is analyzed through 3-D response surface graph by keeping other parameters at middle levels. Interactions of step depth and feed rate on forming time are shown in Fig. 9(a) and (b). It is observed that forming time decreases with increase in step depth and feed rate simultaneously. The contour lines are nearly parallel in diagonal direction. It means high influence of feed rate and step depth on forming time. However, the slope of contour lines of step depth is higher than the slope of feed rate lines, indicating step depth has major impact on forming time than feed rate. Therefore, it is inferred that high step depth and feed rate are required to decrease forming time.

4. Regression Models

The regression model of response is fitted using RSM, and the quadratic model is selected in the present investigation, as given in Eq. 1. The quadratic terms have been used to increase accuracy of the model. (Ref 36)

$$y = \beta_0 + \beta_i \sum x_i + \beta_{ij} \sum x_i x_j + \beta_{ii} \sum x_i^2 + \varepsilon \qquad \text{(Eq 1)}$$

where y = Output response, x_i and x_j = Controllable independent process parameters, β_0, β_i, β_{ij} and β_{ii} = Regression coefficient, and ε = Fitting error.

Regression models for surface roughness and forming time are developed as given in Table 6. These equations are valid for selected material, i.e., aluminum 1050 alloy. The modified regression models are obtained by deleting insignificant terms from the equation. The value of R^2 (pred.) describes the accuracy of regression model. In this study, the value of R^2 (pred.) for surface roughness and forming time is 0.8942 and

0.9957, respectively, which is nearer to 1 and therefore mathematically valid.

From Eq. 2, it is clear that tool size has positive effect while step depth and spindle speed have adverse effect on surface roughness. Tool size is the most dominating term for surface roughness, whereas step depth is the most dominating term for forming time. The graphs of predicted and actual responses are present in Fig. 10. Distribution of points is along straight line, and therefore experimental and predictive values are in good agreement.

5. Optimization of Process Parameters

Forming time reduces with increase in step depth and feed rate. However, surface roughness also increases; therefore, optimization of process parameters is performed to minimize surface roughness and forming time using desirability approach. The desirability function for minimization is calculated using Ref (39).

$$D_f = \left[\frac{h_i - y_i}{h_i - l_i} \right]_i^w \qquad \text{(Eq 4)}$$

where h_i = maximum value of response, l_i = minimum value of response, y_i = corresponding value of response, and w_i = weight of the response.

The optimum levels of process parameters and responses have been determined as given in Table 7.

Figure 11(a) shows the desirability change at optimum level with respect to all process parameters. Desirability of predicted value is near to 1, which means the optimization criterion is acceptable. The bar chart of desirability is shown in Fig. 11(b). Desirability of both responses is also close to 1.

6. Confirmation Tests

Confirmation tests are performed to validate the regression models of surface roughness and forming time, and optimized values of process parameters. Three experiments are performed
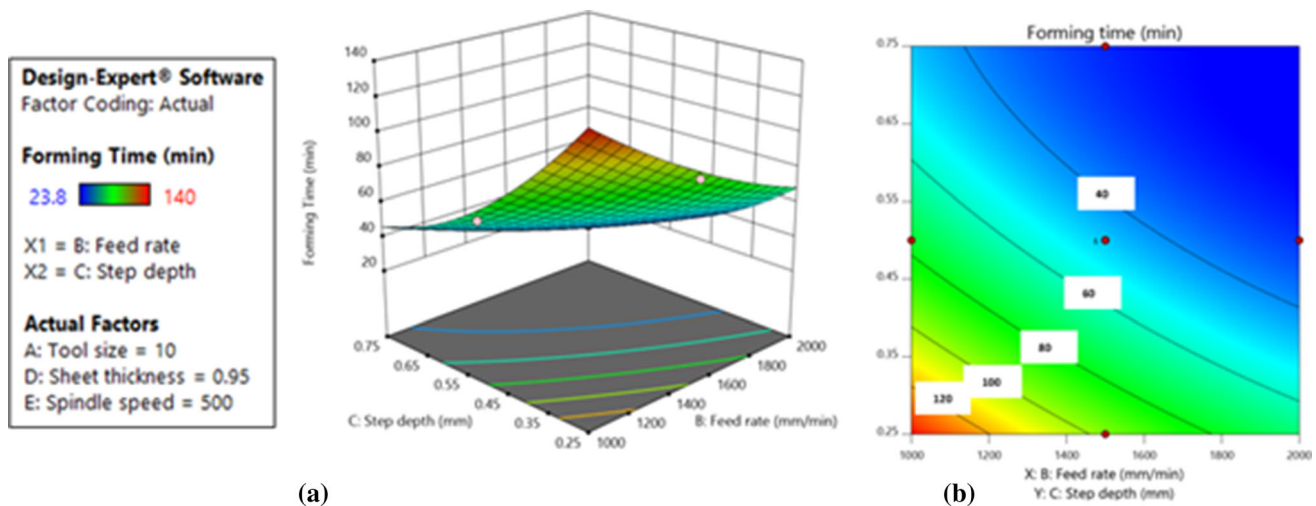

Fig. 9 Response surface graph of interactions for forming time

Table 6 Regression models for surface roughness and forming time

Response	Regression model	Equation number
Surface roughness	$Ra = 29.759 - 5.251 \times A + 9.890 \times C - 8.3888 \times D + 0.0020 \times E - 0.681 \times$ $A \times C + 0.288 \times A \times D - 0.00013 \times A \times E + 0.247 \times A^2$	(2)
Forming time	$Forming\ Time = 392.036 - 0.168 \times B - 528.249 \times C + 0.0925 \times B \times C + 2.5 \times 10^{-5}$ $\times B^2 + 251.7167 \times C^2$	(3)

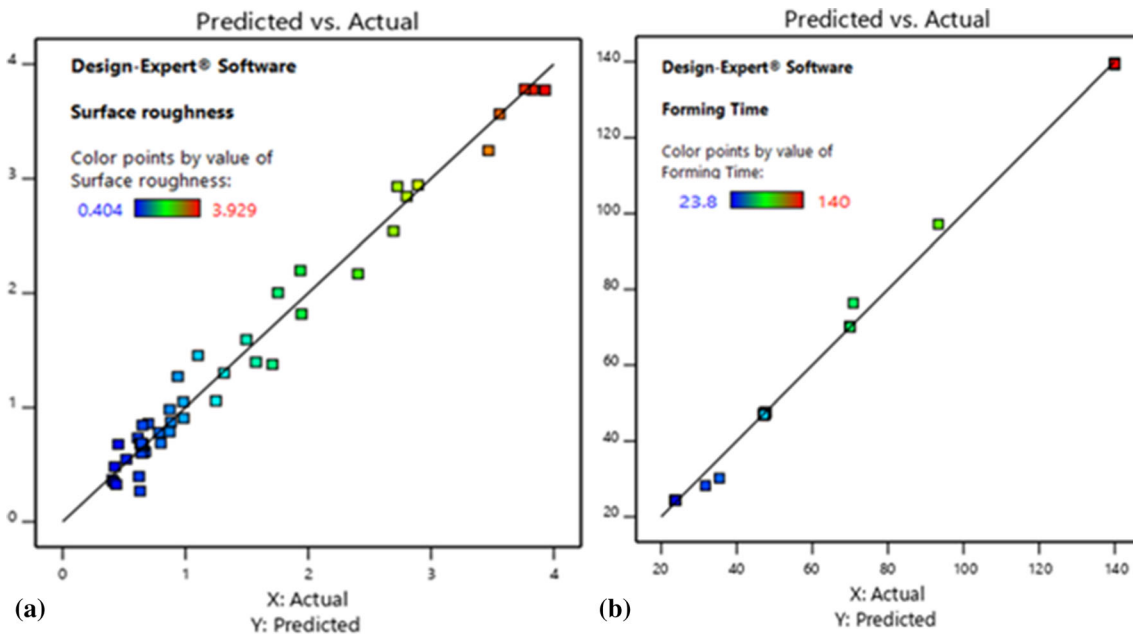where A = Tool size (mm), B = Feed rate (mm/min), C = Step depth (mm), D = Sheet thickness (mm), E = Spindle speed (RPM)

Fig. 10   Contour plot of predicted vs actual values. (a) Surface roughness and (b) forming time

Table 7   Optimization criteria

S. No	Factors	Goal	Lower limit	Upper limit	Optimized value
1	Tool size, mm	In range	8	12	11.45
2	Feed rate, mm/min	In range	1000	2000	1932.64
3	Step depth, mm	In range	0.25	0.75	0.697
4	Sheet thickness, mm	In range	0.7	1.2	0.731
5	Spindle speed rpm	In range	0	1000	44.06
6	Surface roughness, μm	Minimize	0.404	3.929	0.358
7	Forming time, min	Minimize	23.80	140	23.15

to validate regression model, and five tests are conducted to determine the deviation between optimized and observed responses (Ref 40). As given in Table 7, the optimal spindle speed is 44.06 rpm. However, setting spindle speed of 44.06 rpm in existing milling machine is not possible. Therefore for confirmation test, nearest value of spindle speed is selected as 45 rpm. Similarly, sheet thickness is considered as 0.75 mm instead of 0.731 mm. The predicted value for optimum surface roughness and forming time is calculated

considering spindle speed as 45 rpm and sheet thickness as 0.75 mm. The percentage of deviation between predicted and actual value is determined as follows:

$$Deviation(\%) = \frac{|predicted - actual|}{predicted} \times 100 \qquad (Eq\ 5)$$

The results of the confirmation tests are given in Table 8 and 9. Percentage deviation for confirmation tests is less than 10% and therefore acceptable.
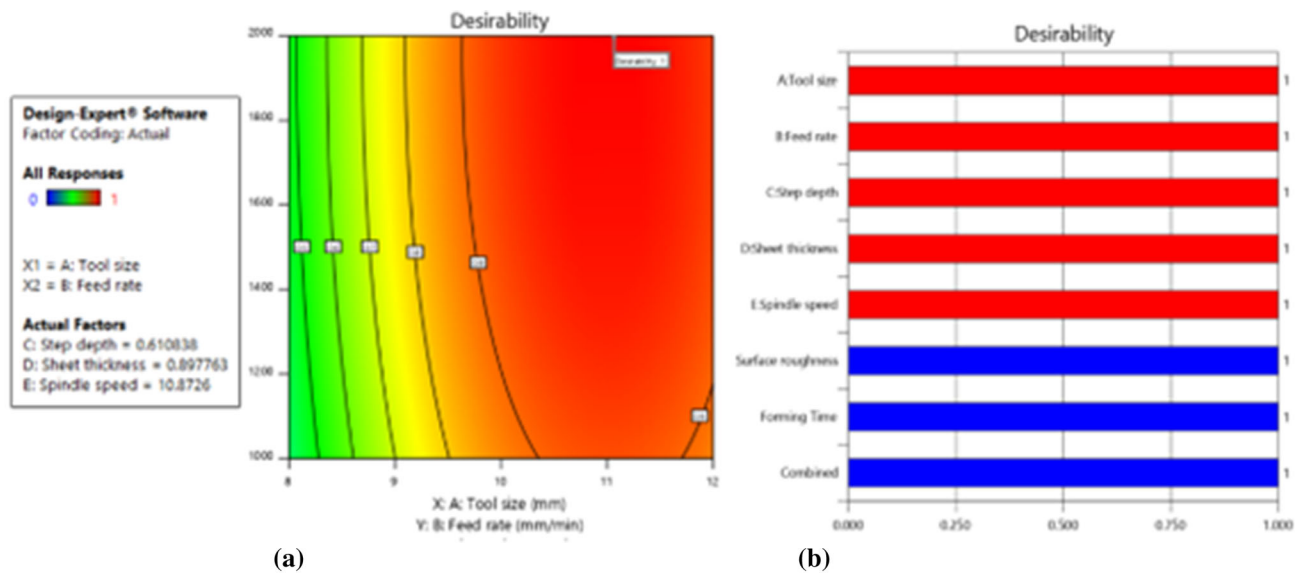
Fig. 11 (a) Desirability plot of optimized process parameters and (b) bar chart of desirability

Table 8 Confirmation results for regression model

| | Process parameters | | | | | Output responses | | | | | |
| | | | | | | Surface roughness | | | Forming time | | |
S. No	Tool size, mm	Feed rate, mm/min	Step depth, mm	Sheet thickness, mm	Spindle speed, RPM	Predicted, μm	Actual, μm	Deviation, %	Predicted, min	Actual, min	Deviation,%
1	14	1700	0.6	1.5	450	4.656	4.235	9.04	33.13	30.92	6.68
2	9	900	0.8	1	250	2.045	2.222	8.61	48.73	49.08	0.71
3	6	700	0.9	0.5	2000	8.345	7.756	6.83	62.71	56.63	9.70

Table 9 Confirmation results for optimized values

| | Surface roughness | | | Forming time | | |
S. No	Predicted, μm	Actual, μm	Deviation, %	Predicted, min	Actual, min	Deviation, %
1	0.353	0.381	7.75	23.76	25.83	8.71
2	0.353	0.387	9.45	23.76	25.83	8.71
3	0.353	0.361	2.09	23.76	25.83	8.71
4	0.353	0.373	5.49	23.76	25.83	8.71
5	0.353	0.358	1.25	23.76	25.83	8.71
Average deviation (%)			5.20			8.71

7. Conclusions

An experimental investigation on surface roughness and forming time of parts formed by MSPIF process has been described in the present paper. The following are the findings of present work:

(i) Tool size is the most significant process parameter influencing surface roughness followed by step depth, spindle speed and sheet thickness. Surface roughness initially decreases and then increases with increase in tool size. It decreases with decrease in step depth, spindle speed and sheet thickness.

(ii) For forming time, step depth is the most significant parameter followed by feed rate. The minimum forming time is observed at maximum level of step depth and feed rate.

Further, regression models are developed to predict average surface roughness and forming time. Also, optimization of process parameters has been performed to minimize surface roughness and forming time. Confirmation tests were performed to validate regression models of surface roughness and

forming time, and optimized values of process parameters. Findings of the present study are useful in effective process planning of MSPIF process.

References

1. S. Golovashchenko and A. Krause, Improvement of Formability of 6xxx Aluminum Alloys Using Incremental Forming Technology, *J. Mater. Eng. Perform*, 2005, **14**(4), p 503–507. https://doi.org/10.1361/105994905X56133
2. P. Shrivastava and P. Tandon, Effect of Preheated Microstructure vis-à-vis Process Parameters and Characterization of Orange Peel in Incremental Forming of AA1050 Sheets, *J. Mater. Eng. Perform*, 2019, **28**(5), p 2530–2542. https://doi.org/10.1007/s11665-019-04032-z
3. J.R. Duflou, J. Verbert, B. Belkassem, J. Gu, H. Sol, C. Henrard, and A.M. Habraken, Process Window Enhancement for Single Point Incremental Forming Through Multi-Step Toolpaths, *CIRP Ann.*, 2008, **57**(1), p 253–256. https://doi.org/10.1016/j.cirp.2008.03.030
4. T.J. Kim and D.Y. Yang, Improvement of Formability for the Incremental Sheet Metal Forming Process, *Int. J. Mech. Sci.*, 2000, **42**(7), p 1271–1286. https://doi.org/10.1016/S0020-7403(99)00047-8
5. Z. Liu, W.J. Daniel, Y. Li, S. Liu, and P.A. Meehan, Multi-Pass Deformation Design for Incremental Sheet Forming: Analytical Modeling, Finite Element Analysis and Experimental Validation, *J. Mater. Process. Technol.*, 2014, **214**(3), p 620–634. https://doi.org/10.1016/j.jmatprotec.2013.11.010
6. J. Jeswiet, F. Micari, G. Hirt, A. Bramley, J. Duflou, and J. Allwood, Asymmetric Single Point Incremental Forming of Sheet Metal, *CIRP Ann.*, 2005, **54**(2), p 88–114. https://doi.org/10.1016/S0007-8506(07)60021-3
7. G. Ambrogio, L. De Napoli, L. Filice, F. Gagliardi, and M. Muzzupappa, Application of Incremental Forming Process for High Customised Medical Product Manufacturing, *J. Mater. Process. Technol.*, 2005, **162**, p 156–162. https://doi.org/10.1016/j.jmatprotec.2005.02.148
8. M. Bambach, B. Taleb Araghi, and G. Hirt, Strategies to Improve the Geometric Accuracy in Asymmetric Single Point Incremental Forming, *Prod. Eng.*, 2009, **3**(2), p 145–56
9. Z. Cui and L. Gao, Studies on Hole-Flanging Process Using Multistage Incremental Forming, *CIRP J. Manuf. Sci. Technol.*, 2010, **2**(2), p 124–128. https://doi.org/10.1016/j.cirpj.2010.02.001
10. L. Junchao, S. Junjian, and W. Bin, A Multipass Incremental Sheet Forming Strategy of a Car Taillight Bracket, *Int. J. Adv. Manuf*, 2013, **69**(9), p 2229–2236. https://doi.org/10.1007/s00170-013-5179-3
11. J. Li, P. Geng and J. Shen, Numerical Simulation and Experimental Investigation of Multistage Incremental Sheet Forming, *Int J Adv Manuf Technol*, 2013, **68**, p 2637–2644
12. N. Moser, E. Ndip-Agbor, H.Q. Ren, Z.X. Zhang, K. Ehmann, and J. Cao, Challenges and Process Strategies Concerning Multi-Sided Double Sided Incremental Forming, *Key Eng. Mater.*, 2015, **651**, p 1122–1127. https://doi.org/10.4028/www.scientific.net/KEM.651-653.1122
13. J. Verbert, B. Belkassem, C. Henrard, A.M. Habraken, J. Gu, H. Sol, B. Lauwers, and J.R. Duflou, Multi-Step Toolpath Approach to Overcome Forming Limitations in Single Point Incremental Forming, *Int. J. Mater. Form.*, 2008, **1**, p 1203–1206. https://doi.org/10.1007/s12289-008-0157-2
14. R. Malhotra, A. Bhattacharya, A. Kumar, N.V. Reddy, and J. Cao, A New Methodology for Multi-Pass Single Point Incremental Forming with Mixed Toolpaths, *CIRP Ann.*, 2011, **60**(1), p 323–326. https://doi.org/10.1016/j.cirp.2011.03.145
15. L. Manco, L. Filice, and G. Ambrogio, Analysis of the Thickness Distribution Varying Tool Trajectory in Single-Point Incremental Forming, *Proc. Inst. Mech. Eng. B. J. Eng. Manuf.*, 2011, **225** (3), p 348–56

16. J. Li, J. Hu, J. Pan, and P. Geng, Thickness Distribution and Design of a Multi-Stage Process for Sheet Metal Incremental Forming, *Int. J. Adv. Manuf. Technol.*, 2012, **2**(9), p 981–988. https://doi.org/10.1007/s00170-011-3852-y
17. Z. Liu, Y. Li, and P.A. Meehan, Tool Path Strategies and Deformation Analysis In Multi-Pass Incremental Sheet Forming Process, *Int. J. Adv. Manuf. Technol.*, 2014, **5**(1), p 395–409. https://doi.org/10.1007/s00170-014-6143-6
18. X. Shi, G. Hussain, G. Zha, M. Wu, and F. Kong, Study on Formability of Vertical Parts Formed by Multi-Stage Incremental Forming, *Int. J. Adv. Manuf. Technol.*, 2014, **75**(5), p 1049–1053. https://doi.org/10.1007/s00170-014-6192-x
19. Z. Li, S. Lu, T. Zhang, Z. Mao, and C. Zhang, Analysis of Geometrical Accuracy Based on Multistage Single Point Incremental Forming of a Straight Wall Box Part, *Int. J. Adv. Manuf. Technol.*, 2017, **93**(5), p 2783–2789. https://doi.org/10.1007/s00170-017-0723-1
20. S. Wu, Y. Ma, L. Gao, Y. Zhao, S. Rashed, and N. Ma, A Novel Multi-Step Strategy Of Single Point Incremental Forming for High Wall Angle Shape, *J. Manuf. Process.*, 2020, **56**, p 697–706. https://doi.org/10.1016/j.jmapro.2020.05.009
21. H.K. Nirala, P.K. Jain, J.J. Roy, M.K. Samal, and P. Tondon, An Approach to Eliminate Stepped Features in Multistage Incremental Sheet Forming Process: Experimental and FEA Analysis, *J. Mech. Sci. Technol*, 2017, **31**(2), p 599–604. https://doi.org/10.1007/s12206-017-0112-6
22. M. Shamsari, M.J. Mirnia, M. Elyasi, and H. Baseri, Formability Improvement in Single Point Incremental Forming of Truncated Cone Using a Two-Stage Hybrid Deformation Strategy, *Int. J. Adv. Manuf*, 2018, **94**(5), p 2357–2368. https://doi.org/10.1007/s00170-017-1031-5
23. P. Dai, Z. Chang, M. Li, and J. Chen, Reduction of Geometric Deviation by Multi-Pass Incremental Forming Combined with Tool Path Compensation for Non-Axisymmetric Aluminum Alloy Component with Stepped Feature, *Int. J. Adv. Manuf*, 2019, **102**(1), p 809–817. https://doi.org/10.1007/s00170-018-3194-0
24. E. Ndip-Agbor, P. Cheng, N. Moser, K. Ehmann, and J. Cao, Prediction of Rigid Body Motion in Multi-Pass Single Point Incremental Forming, *J. Mater. Process. Technol.*, 2019, **269**, p 117–127. https://doi.org/10.1016/j.jmatprotec.2019.02.007
25. M. Skjoedt, M.B. Silva, P.A. Martins, and N. Bay, Strategies and Limits in Multi-Stage Single-Point Incremental Forming, *J. Strain Anal. Eng. Des.*, 2010, **45**(1), p 33–44
26. S. Gajjar, V. Sisodia, R. Jagtap, K. More, and S. Kumar Experimental investigation on geometric accuracy and surface roughness of formed part in multistage single point incremental forming (spif) process, In Innovative Design, 2021. https://doi.org/10.1007/978-981-15-6619-6_22
27. H. Lu, H. Liu, and C. Wang, Review on Strategies for Geometric Accuracy Improvement in Incremental Sheet Forming, *Int. J. Adv. Manuf*, 2019, **102**(9), p 3381–3417. https://doi.org/10.1007/s00170-019-03348-3
28. I. Cerro, E. Maidagan, J. Arana, A. Rivero, and P.P. Rodriguez, Theoretical and Experimental Analysis of the Dieless Incremental Sheet Forming Process, *J. Mater. Process. Technol.*, 2006, **177**(1–3), p 404–408
29. O.U. Lasunon, Surface Roughness in Incremental Sheet Metal Forming of AA5052, *Adv. Mater. Res.*, 2013, **753**, p 203–206
30. C. Raju and C.S. Narayanan, Application of a Hybrid Optimization Technique in a Multiple Sheet Single Point Incremental Forming Process, *Measurement*, 2016, **78**, p 296–308
31. A. Mulay, S. Ben, S. Ismail, and A. Kocanda, Experimental Investigations into the Effects of SPIF Forming Conditions on Surface Roughness and Formability by Design of Experiments, *J. Braz. Soc. Mech. Sci. Eng.*, 2017, **39**(10), p 3997–4010. https://doi.org/10.1007/s40430-016-0703-7
32. H.R. Dodiya, D.A. Patel, A.B. Pandey, D.D. Patel, and S. Saladi, Experimental Investigation of Surface Roughness for AA3003-0 Aluminium Alloy Using Single Point Incremental Forming, *Mater. Today: Proc*, 2021, **46**, p 8655–8662

33. S. Zhang, G.H. Tang, Z. Li, X. Jiang, and K. Li, Experimental Investigation on the Spring Back of AZ31B Mg Alloys in Warm Incremental Sheet Forming Assisted with oil Bath Heating, *Int. J. Adv. Manuf*, 2020, **109**(1), p 535–551

34. J. Antony, *Design of Experiments for Engineers and Scientists*, Elsevier, New York, 2014

35. H.B. Lu, Y.L. Li, Z.B. Liu, S. Liu, and P.A. Meehan, Study on Step Depth for Part Accuracy Improvement in Incremental Sheet Forming Process, *J. Adv. Mater. Res.*, 2014, **939**, p 274–280

36. P. Gupta and J. Jeswiet, Effect of Temperatures During Forming In Single Point Incremental Forming, *Int. J. Adv. Manuf.*, 2018, **95**(9), p 3693–3706

37. Z. Chang and J. Chen, Analytical Model and Experimental Validation of Surface Roughness for Incremental Sheet Metal Forming Parts, *Int. J. Mach. Tools Manuf.*, 2019, **146**, p 103453

38. G. Palumbo and M. Brandizzi, Experimental Investigations on the Single Point Incremental Forming of a Titanium Alloy Component Combining Static Heating with High Tool Rotation Speed, *Mater. Des*, 2012, **40**, p 43–51

39. AI Khuri 2006 Response surface methodology and related topics, World scientific

40. W.A. Jensen, Confirmation Runs in Design of Experiments, *J. Qual. Technol.*, 2016, **48**, p 162–177. https://doi.org/10.1080/00224065.2016.11918157